Spectroscopic Characterization of Oligoaniline Microspheres Obtained by an Aniline−Persulfate Approach

ARTICLE *in* THE JOURNAL OF PHYSICAL CHEMISTRY B · FEBRUARY 2011

Impact Factor: 3.3 · DOI: 10.1021/jp111065m · Source: PubMed

3 AUTHORS, INCLUDING:

Daniela Colevati Ferreira
Institute of Tecnological Research from Stat…
15 PUBLICATIONS **143** CITATIONS
SEE PROFILE

José Ricardo Pires
Federal University of Rio de Janeiro
30 PUBLICATIONS **582** CITATIONS
SEE PROFILE

THE JOURNAL OF PHYSICAL CHEMISTRY B

ARTICLE

pubs.acs.org/JPCB

Spectroscopic Characterization of Oligoaniline Microspheres Obtained by an Aniline−Persulfate Approach

Daniela C. Ferreira,[†] José R. Pires,[‡] and Marcia L. A. Temperini*[,†]

[†]Departamento de Química Fundamental, Instituto de Química, Universidade de São Paulo, CP 26077 CEP 05513-970, São Paulo, SP, Brasil

[‡]Instituto de Bioquímica Médica, Centro de Ciências da Saúde, Universidade Federal do Rio de Janeiro, 21941-590, Rio de Janeiro, RJ, Brasil

Supporting Information

ABSTRACT: This paper investigates the structure of the products obtained from the polymerization of aniline with ammonium persulfate in a citrate/phosphate buffer solution at pH 3 by resonance Raman, NMR, FTIR, and UV−vis−NIR spectroscopies. All the spectroscopic data showed that the major product presented segments that were formed by a 1,4-Michael reaction between aniline and *p*-benzoquinone monoimine, ruling out the formation of polyazane structure that has been recently proposed. The characterization of samples obtained at different stages of the reaction indicated that, as the reaction progressed, phenazine units were formed and 1,4-Michael-type adducts were hydrolyzed/oxidized to yield benzoquinone. Raman mapping data suggested that phenazine-like segments could be related to the formation of the microspheres morphology.

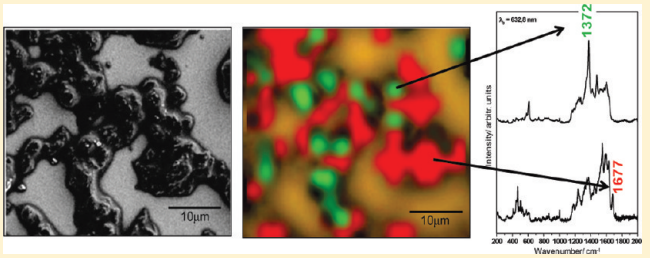

1. INTRODUCTION

Polyaniline (PANI) is one of the most important conducting polymers due to its straightforward synthesis, good stability, and various technological applications.[1−3] The conducting form of PANI, the emeraldine salt (PANI-ES), presents semiquinone radical cations (polarons) in the chain which are formed by a head-to-tail coupling of aniline monomers, as shown in Scheme 1A.

The design and fabrication of nano/microstructured PANI has been attracting a great deal of interest since their properties are likely to exhibit improved electrical, optical, and chemical properties as compared to their bulk counterparts.[4,5] In order to obtain nano/microstructured materials, many methods have been reported based on variations in the standard oxidative polymerization of aniline with ammonium persulfate (APS) protocol. In this context, the main routes for obtaining nanoscaled PANI-ES are the chemical polymerization of aniline by APS in the presence of template,[6,7] by forcing the polymerization at an aqueous−organic interface,[8] and/or by changing the pH of the polymerization medium.[9−14] However, the reaction mechanisms and the identity of the intermediates produced from these routes are still subject of discussion. It is clear that the characterization of their structure as well as the mechanistic understanding of these reactions is imperative to optimize the synthesis strategies, which in turn can enable the design and preparation of nano/microstructured PANI with controllable size, morphology, and structure. This could allow, for example, one to tailor its characteristics to enhance properties for a target application.

Recently, a study by Venancio et al. regarding the role of pH on the morphology of the product involved the polymerization of aniline with APS using citrate/phosphate buffer solutions at pH 3.0 and 4.0 led to the formation of hollow microspheres.[9] Based on UV−vis, FTIR, and ^{1}H-RMN, it was proposed the microspheres are formed by polyazane chains in which the aniline units are connected via N−N bonds and having benzoquinone units as side group (as shown in Scheme 1B). However, Surwade et al. proposed an alternative reaction scheme for the chemical oxidative polymerization of aniline with APS in aqueous pH 2.5−10 buffers, in which the products are composed of a mixture of Michael-type adducts of benzoquinone monoimine and aniline at various stages of hydrolysis (Scheme 1C).[10] It is worth pointing out that these syntheses were performed exactly as described by Venancio et al.

Herein, we aim at employing resonance Raman and NMR spectroscopies to gain further insight into structure of the products obtained by the aforementioned protocol, i.e., aniline/APS polymerization in a buffer solution at pH 3. Resonance Raman spectroscopy is very attractive to this end due to its selectivity and sensitivity to chromophore segments in polymeric chains, enabling a clear distinction regarding the formation of either polyazane chains or Michael-type adducts of benzoquinone monoimine and aniline.

2. EXPERIMENTAL SECTION

2.1. Preparation of Citrate/Phosphate Buffer Solution at pH 3. The citrate/phosphate buffer aqueous solution (pH 3)

Received: November 19, 2010
Revised: December 28, 2010
Published: January 26, 2011

Scheme 1. Schematic Representation (A) Esmeraldine Salt, Conducting Form of PANI; (B) Polyazane;[9] and (C) 1,4-Michael-Type Adducts[10]

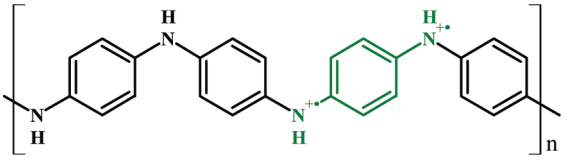

(A)

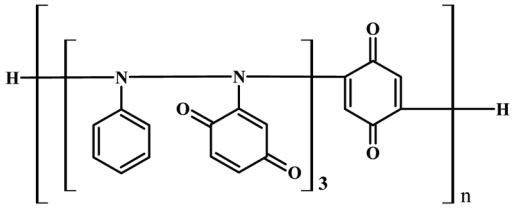

Polyazane

(B)

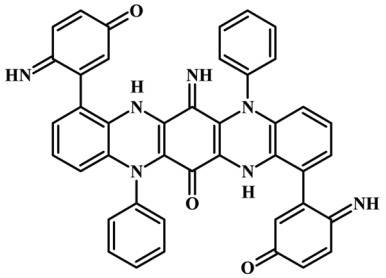

Michael-type adduct

(C)

was prepared by mixing 320 mL of a 0.1 M citric acid (99%, Sigma-Aldrich) aqueous solution and 80 mL of a 0.2 M disodium hydrogen phosphate (99.5%, Vetec) aqueous solution.

2.2. Synthesis of Oligoaniline Microspheres at pH 3. Aniline (99%, Aldrich) was distilled under reduced pressure prior to use. In a typical synthesis,[9] 360 μL of aniline (4.0 mmol) and 0.9 g of APS (4.0 mmol) were separately dissolved in 200 mL of citrate/phosphate buffer solution each and added to a 600 mL glass beaker. After 2 min of mixing, the pH of the solution was measured (pH 3) and this value was assumed as being the initial pH in the polymerization process. Five aliquots of 80 mL each were transferred to five different Erlenmeyer flasks. The flasks were capped and sealed with parafilm and left undisturbed. 140 mL of 1.0 M ammonium hydroxide aqueous solution was added to each flask in order to quench the reaction after 5.5, 22, 49, 102, and 171 h of polymerization for flasks 1 through 5, respectively, yielding samples T5.5−T171. No changes in pH were detected during the reaction. The filtration of the solid must be quickly done in order to suppress any aniline oxidation in alkaline solution. The precipitate, a yellowish brown solid, was collected and washed with aqueous solution 1.0 M ammonium hydroxide until the observation of a colorless filtered solution. The solids were then dried under vacuum at room temperature.

2.3. Synthesis of Oligoaniline Using 1,4-Benzoquinone as Oxidant Agent. 1,4-Benzoquinone (99%, Riedel-de-Haën) was purified by sublimation prior to use. The synthesis of oligoaniline using 1.4-benzoquinone as oxidant was carried out as described by Surwade et al.[10] Briefly, 2 mL of aniline (22 mmol) was dissolved in 200 mL of 1.0 M HCl (37%, Synth) aqueous solution in a 400 mL round-bottom flask with a magnetic stirrer, followed by addition of 0.1 g of 1,4-benzoquinone (9.2 mmol). After 1 h stirring, the product was isolated by filtration. The dark brown solid was washed with deionized water until the observation of a colorless filtered solution and dried under vacuum at room temperature. This solid was labeled AnBzq.

2.4. Instrumentation. The electronic UV−vis−NIR spectra were recorded on a Shimadzu UV3101PC. FTIR spectra of samples dispersed in KBr pellets were recorded on a Bomen MB100 with a resolution of 4 cm^{-1}. Raman spectra at 413 nm (Kr^+, Coherent INNOVA 90-6) exciting wavelength were recorded in a Jobin Yvon (T64000) triple spectrometer with CCD detector. The laser power at the sample was ca. 10−15 mW and to avoid local heating the sample was dispersed in K_2SO_4 (1:50 ratio in weight). The Raman spectra and Raman mapping at 633 nm (He−Ne, Renishaw 7N1753) exciting wavelength were recorded in a Renishaw Raman imaging microscope (in Via) containing a Leica microscope and a CCD detector. The Raman mapping was recorded with a 1200 lines/mm grating in static mode centered at 1600 cm^{-1} and a 100× objective (NA = 0.85) with a circular laser spot at the sample. The step size used in mapping was 3.5 μm in both directions of the plane of the slide. The mapping was built up by fitting a mixed Gaussian−Lorentzian curve to the Raman bands at ca. 1370 and 1680 cm^{-1} and measuring the peak intensity after background subtraction using Wire 3.1 software. In order to quench the fluorescence, the Raman spectrum of safranine-O (Merck) and AnBzq and the Raman mapping at 633 nm exciting radiation were obtained on a glass slide coated with smooth Au film (80 nm thick) deposited by sputtering (Edwards Scancoat Six, FTM6). Scanning electron micrographs of uncoated samples were recorded on a field emission scanning electron microscope JEOL JSM-7401 using a voltage of 1.0−5.0 kV. To obtain the mass curves, the samples were diluted to a concentration ~5 mg/mL in tetrahydrofuran (99%, Vetec) and analyzed by ion trap LC-MS-Bruker Daltonic Esquire 3000 Plus coupled to a high-performance liquid chromatograph. ^1H and ^{13}C NMR spectra were acquired in a Bruker AVIII 800 spectrometer, 800.4 MHz proton, 201.3 MHz carbon frequencies, equipped with an inverse triple-resonance TXI probe with Z-gradient. Saturated DMSO-d_6 solutions of the samples were used for the NMR analysis, at 298 K. The spectra acquired were the following: 1D ^1H NMR (number of scans = 8, relaxation delay = 5 s, FID points = 4096); 2D $^1H-^{13}C$ HMQC[15] (number of scans = 4, relaxation delay = 5 s, FID points = 1024 × 512) and 2D DOSY[16] (number of scans = 8, relaxation delay = 5 s, FID points = 16 384, gradient pulse length δ = 2 ms, diffusion delay Δ = 100 ms, gradient field incremented linearly in 16 steps from 0.67 to 32 G cm^{-1}. The NMR experiments above were performed for all samples. Additionally, for samples obtained in buffer pH = 3 and reaction time 5.5 h the following spectra were acquired: 1D ^{13}C APT[17] (number of scans = 8528, relaxation delay = 2 s, FID points = 65 536) and 2D $^1H-^1H$ TOCSY[18] (number of scans = 40, relaxation delay = 5 s, FID points = 4096 × 2048, spin-lock = 35 ms).

dx.doi.org/10.1021/jp111065m |J. Phys. Chem. B 2011, 115, 1368–1375

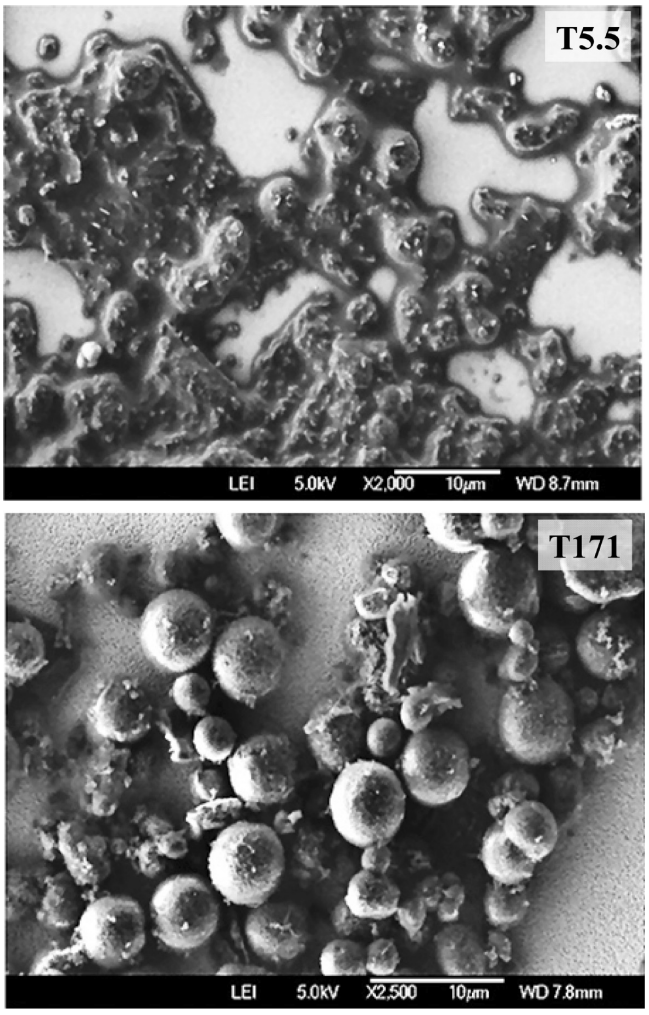

Figure 1. SEM images of the T5.5 and T171 products.

3. RESULTS AND DISCUSSION

Figure 1 shows SEM images of T5.5 (top) and T171 (bottom). It can be observed in T171 the formation of microspheres with diameter size in the range of ca. 2−7 μm, while T5.5 has an irregular morphology. The molecular weights of T5.5 and T171 samples dissolved in THF and previously separated by HPLC were determined by ESI-TOF-MS. Both samples were eluted as a single broad peak centered at retention time of 3.2 min and presents molecular weight in the range 600−1000, in accordance to the literature.[10] The two samples exhibited the same mass curve pattern with two main peaks at 974.5 and 663.5 m/z, indicating that mixtures comprising similar components were obtained regardless of the reaction time. The major component in both reaction times had a 974.5 m/z, while the increase of the peak at 663.5 m/z in T171 suggests an enrichment of this compound in the mixture.

Figure 2 shows the UV−vis−NIR spectra (*N*-methylpyrrolidone solution) of the products T5.5−171. One can see that all products present similar absorption spectra (two strong bands at ca. 275 and 370 nm and a very weak band at ca. 510 nm), in accordance with the spectra obtained by the polymerization of aniline in mild acidic medium.[9,10,19−23] However, a subtle change was observed in the electronic spectra with the increase of the reaction time: the bands at ca. 275 and 370 nm (T5.5) are

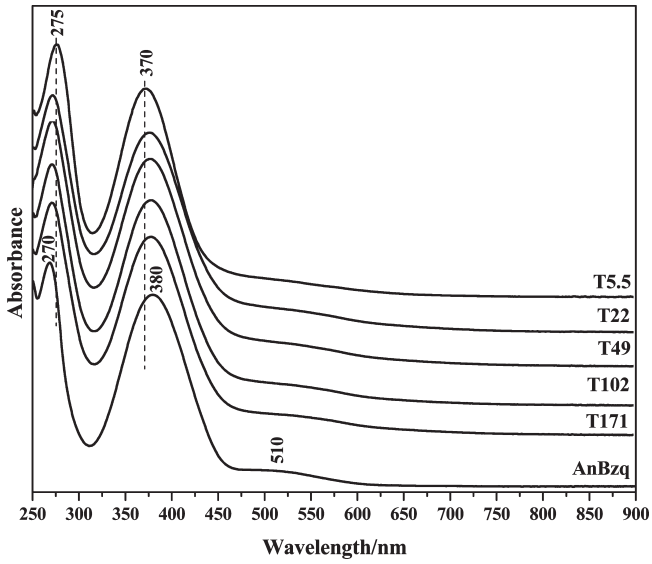

Figure 2. UV−vis−NIR spectra of T5.5−171 samples and AnBzq.

displaced to ca. 270 and 380 nm (T171), respectively, after 22 h of reaction and there is a slight intensification of the band at ca. 510 nm. After this spectral evolution, no other variation was observed over time. Figure 2 also shows the spectrum of the product formed from the reaction between aniline and 1,4-benzoquinone. This product, named AnBzq, was proposed to have the same structure as the products of the aniline−APS reaction at pH 3.[10] It should be noted that the all UV−vis−NIR spectra (T5.5−171) are very similar to the spectrum of AnBzq.

Figure 3 shows the Raman spectra of T5.5−171 and AnBzq (excitation of 413 nm). It is worth noting that the 413 nm laser line was chosen to attain a preresonance condition with the electronic absorption at 380 nm (see Figure 2). As the reaction time increased, there was a progressive decrease of the intensities of the bands at ca. 1540 and 1580 cm^{-1}. Conversely, the Raman spectrum of T171 is quite similar to the Raman spectrum of AnBzq (Figure 3), where the Raman bands at ca. 1540 and 1580 cm^{-1} are absent or very weak. The decrease in the intensity of these bands can be related to the hydrolysis/oxidation of benzoquinone monoimine units to benzoquinone over time, indicating the formation of a chromophore formed by 1,4-Michael-type reactions between aniline and *p*-benzoquinone monoimine as the reaction progressed. This data is supported by FTIR and elemental analysis (see Supporting Information).

We also investigated the resonance Raman spectra of T5.5−T171 employing 633 nm excitation radiation, as shown in Figure 4. It is well-known that phenazine segments are in resonance with this excitation line.[24−26] The Raman spectra of T5.5−T171 and AnBzq exhibited a high fluorescence background. In order to quench this fluorescence, Raman spectra were recorded on a smooth gold surface (80 nm thick). Figure 4A,B shows the spectra recorded for two different regions in sample T5.5. It can be noted that the spectra profiles were different. In Figure 4A, bands at 466 and 1680 cm^{-1} were detected. These signals are assigned to carbonyl groups and are also detected in the AnBzq Raman spectrum (Figure 4D). On the other hand, bands at ca. 610 and 1370 cm^{-1} were observed for T5.5 (Figure 4B) and T171 (Figure 4C). They can be assigned to δ_{ring} and ν_{C-N+} vibrations which were also observed in the safranine-O spectrum (Figure 4E) and are associated with the presence of phenazine-like segments. It is

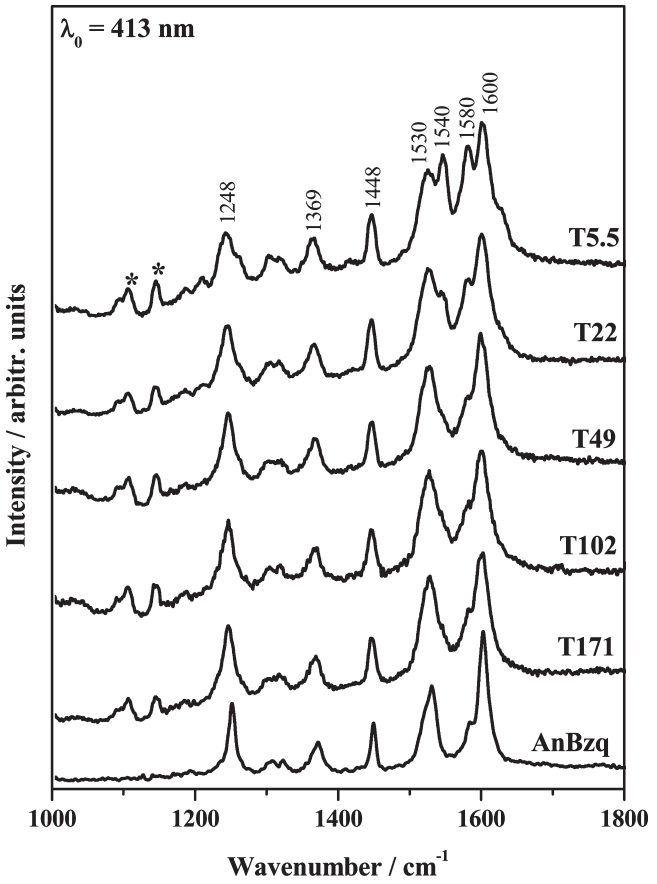

Figure 3. Raman spectra (λ_0 = 413 nm) of T5.5−T171 and AnBzq. The Raman bands indentified by asterisks refer to SO_4^{2-} anions (sample/K_2SO_4 = 1:50).

important to note that we also detected a mixture of these two spectral profiles in some regions of T5.5. However, only phenazine-like spectral profile was observed for T171.

In order to further investigate the structure of the products obtained at different reaction times, several NMR spectra were acquired. Figure 5 shows 1D ^{1}H NMR spectra of T5.5 (red), T171 (blue), and AnBzq (green) and a superposition of the 2D DOSY spectra of these three samples. The ^{1}H NMR spectra of T5.5 and T171 show resonances in three regions: (i) in 5.4−6.4 ppm, signals that could be assigned to alkenes as in the benzoquinone or benzoquinone monoimine moieties; (ii) in 6.6−7.6 ppm, signals that could be assigned to aromatics; and (iii) in 8.5−10.5, signals assigned to nitrogen-bonded hydrogens.

From the 2D DOSY experiment (Figure 5) we get diffusion coefficients in the range of $(4.1-3.1) \times 10^{-10}$ m^2/s ($\log D = -9.38$ to -9.51) for AnBzq, and in the range of $(2.8-3.2) \times 10^{-10}$ m^2/s ($\log D = -9.48$ to -9.55) and $(2.2-2.8) \times 10^{-10}$ m^2/s ($\log D = -9.55$ to -9.65) for the T5.5 and T171 samples, respectively. The DOSY spectra suggest that in the course of the oxidative polymerization at pH 3, only small changes in molecular size occurred from 5.5 to 171 h. Nevertheless, for sample T171, a smaller diffusion coefficient was measured relative to T5.5, suggesting that the sample T171 becomes more aggregated. This observation is in agreement with the Raman spectra (Figure 4) that indicated the formation of phenazine-like segments with increasing reaction times. As phenazine-like segments have a planar geometry, they may interact by π-stacking, resulting in a higher aggregation degree. Aggregation is suggested by the fact that only a relatively broad range of diffusion coefficients are measured for each sample instead of discrete diffusion coefficients for each component of the sample. For AnBzq, a higher diffusion coefficient was observed than for T5.5 and T171. This result may be associated with a lower aggregation

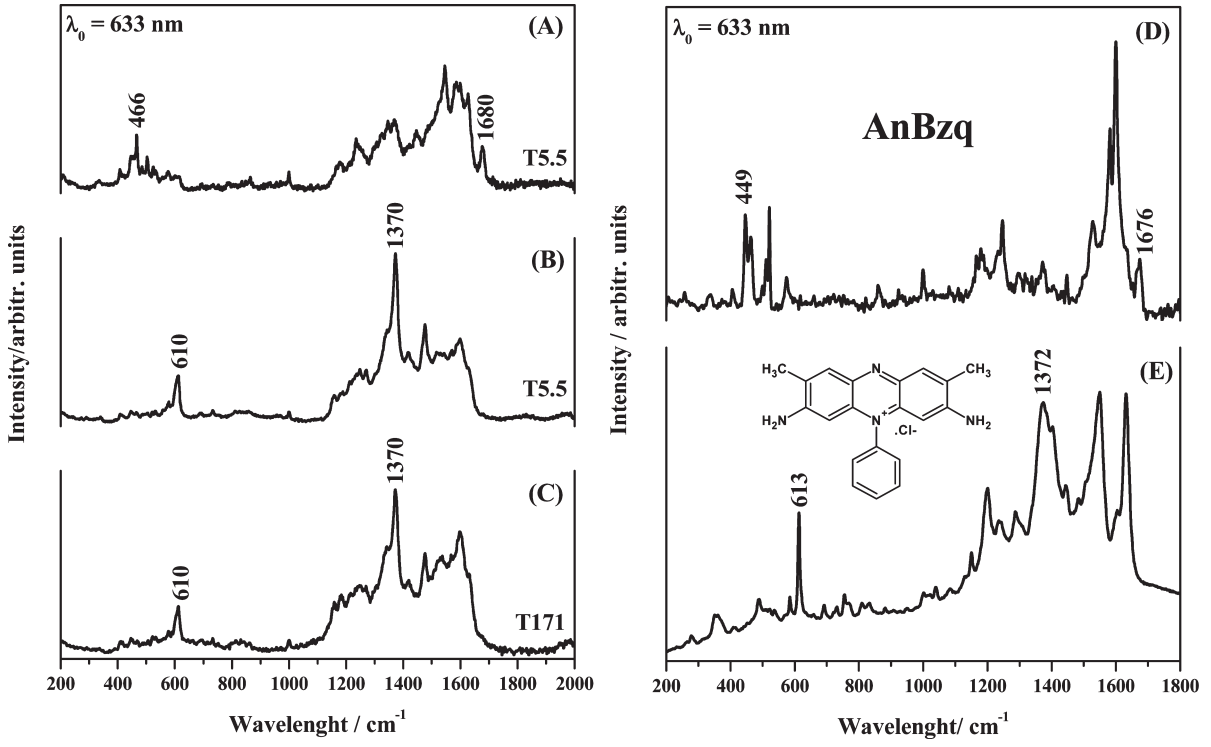

Figure 4. (A,B) Raman spectra (λ_0 = 633 nm) of T5.5 sample. While in (A), a 1,4-Michael-type reaction product spectrum profile is observed, (B) contains a phenazine-like profile. (C−E) Raman spectra (λ_0 = 633 nm) of (C) T171, (D) AnBzq, and (E) safranine-O.

dx.doi.org/10.1021/jp111065m |J. Phys. Chem. B 2011, 115, 1368–1375

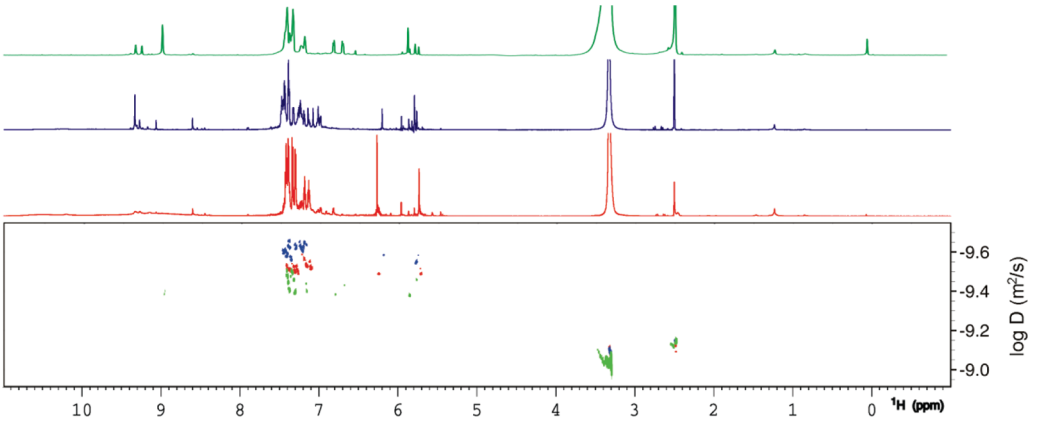

Figure 5. ^{1}H NMR spectra in DMSO-d_6 at 298 K of samples T5.5 (red), T171 (blue), and AnBzq (green) and a superposition of the 2D DOSY spectra of these three samples.

degree due to the absence of phenazine-like segments in AnBzq structure.

Comparison of the ^{1}H NMR spectra of the samples T5.5 and T171 reveals some important differences. First, the broad signals occurring at chemical shifts around 8.5−10.5 ppm assigned to hydrogens bonded to nitrogen are replaced by a number of sharper signals; this fact correlates with the disappearance in the IR spectrum (showed in the Supporting Information) of the band at 3265 cm^{-1} assigned to the N−H stretching with the increase of the reaction time. Also, aromatic ^{1}H signals shift downfield with increasing reaction time, supporting the hydrolysis of the benzoquinone monoimine to benzoquinone or the formation of phenazine-like segments since the substitution of N by O in the benzoquinone monoimine units as well as the formation of a charged N^{+} in the phenazine moiety would lead to electronic withdrawal in the conjugated aromatic rings. Finally, changes in the alkene hydrogen signals were detected, suggesting modifications of the benzoquinone monoimine moiety. The signals related to the aromatic and alkene hydrogens were analyzed in detail using homonuclear (TOCSY) and heteronuclear (^{13}C HMQC) correlation spectroscopy (Figures 6 and 7). Inspection of the aromatic region of the ^{1}H NMR spectrum (6.6−7.6 ppm) using homonuclear and heteronuclear correlation NMR spectroscopy reveals a number of aromatic rings with different substitution patterns (Figure 6). The signals labeled 1 in the figure (two triplets and one doublet) can be assigned to a monosubstituted benzenic ring; this system is composed of a doublet (assigned to hydrogens $H_{2,6}$ of the aromatic ring which are coupled with hydrogens $H_{3,5}$ and thus yielding a doublet with $J_{2,3}$ ca. 8 Hz), a triplet (assigned to hydrogens $H_{3,5}$ of the aromatic ring which are coupled with hydrogens $H_{2,6}$ and to hydrogen H_4 thus yielding a triplet with $J_{3,2}$ and $J_{3,4}$ ca. 8 Hz), and a weaker triplet (assigned to hydrogen H_4, which is coupled to hydrogens $H_{3,5}$ thus yielding a triplet with $J_{4,3}$ and $J_{4,5}$ ca. 8 Hz). The signals labeled 2 have the same pattern of the signals labeled 1 and can also be assigned to a monosubstituted benzenic ring, but in a different environment than the benzenic ring 1.

Signals labeled 3, 4, 5, and 6 are smaller in intensity comparatively to signals labeled 1 and 2, and were assigned to benzenic rings with a 1,2,4 three-substitution pattern (signals labeled 3, 5, 6) or 1,4- or 1,2-bisubstituted benzenic rings (signals labeled 4).

Comparison of the spectra obtained for the samples T5.5 (Figure 6, red) and T171 (blue) showed some differences. The signals labeled 1 and 2 are absent in the sample obtained in longer reaction times. Instead, we observed the signals labeled 8, which were weak signals at shorter reaction time, but become stronger in longer reaction times, and the signals labeled 8 were assigned to monosubstituted benzenic rings. The same occurs for signals labeled 3 and 4 which are observed only in the samples obtained at short reaction times, while the signals 5, 6, and 7 became more intense in the sample obtained at longer reaction times.

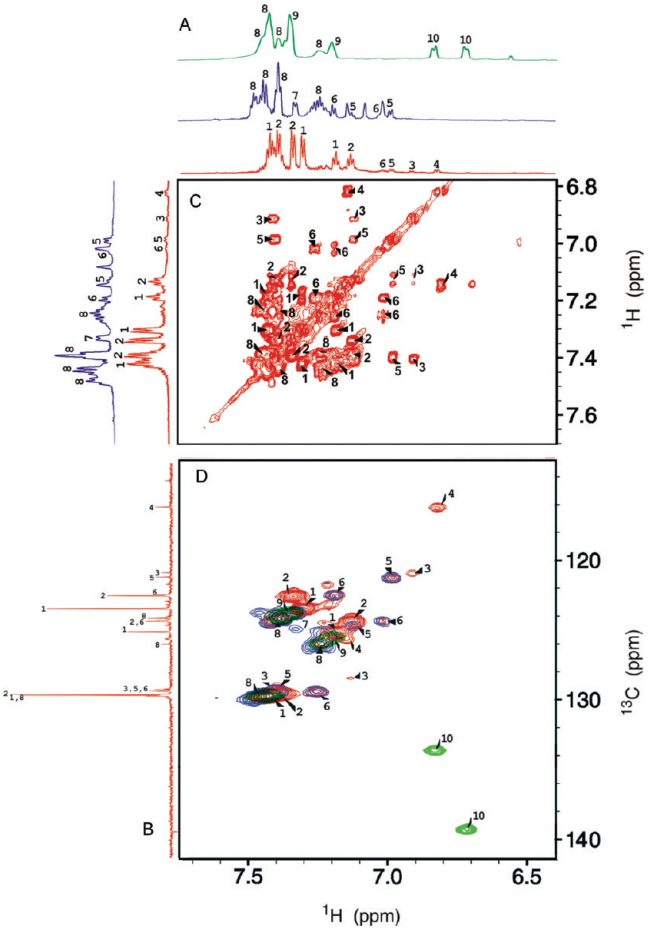

Figure 6. NMR analysis of the samples T5.5 (red), T171 (blue), and AnBzq (green) using homonuclear and heteronuclear correlation spectroscopy. Aromatic region (A) ^{1}H, (B) ^{13}C APT, (C) ^{1}H−^{1}H TOCSY, and (D) ^{1}H−^{13}C HMQC spectra.

dx.doi.org/10.1021/jp111065m |J. Phys. Chem. B 2011, 115, 1368–1375

At longer reaction times we also observe the appearance of some singlet signals at 6.6−7.6 ppm, which can be attributed to N-bounded hydrogens considering that no corresponding signals are observed at the ^{13}C HMQC spectrum.

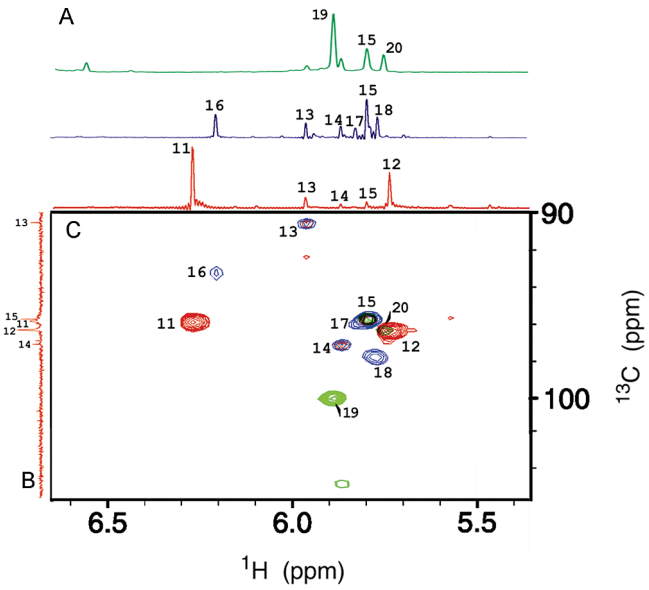

Figure 7. NMR analysis of the T5.5 (red) and T171 (blue) samples and AnBzq (green) using heteronuclear correlation spectroscopy. Alkene region (A) ^{1}H, (B) ^{13}C APT, and (C) $^{1}H-^{13}C$ HMQC spectra.

The signals labeled 8 are also present in the product of the reaction of *p*-benzoquinone and aniline (AnBzq) (Figure 6). The signals labeled 9 in AnBzq have very similar chemical shifts to the signals labeled 1 for T5.5, suggesting that the aromatic rings 1, 8, and 9 are in the vicinity of the carbonyl of the benzoquinone or benzoquinone monoimine, while the aromatic ring labeled 2, which occurs only in T5.5, could be assigned to an aromatic ring in the vicinity of the imino group of the benzoquinone monimine. The course of the reaction of aniline verifies that the benzoquinone monoimine units initially formed are converted into benzoquinone as suggested by the disappearance of signals labeled 2 and rising of the signals labeled 8 and 9.

The alkene region 5.4−6.4 ppm (Figure 7) shows a number of singlet signals numbered 11−18. These signals were attributed to benzoquinone or benzoquinone monoimine moieties. The signals 11 and 12 appear only in the T5.5 sample while the signals 13−18 become more intense in the T171 sample. For AnBzq the signal 15 and the signal labeled 20, which are very similar to the signal labeled 12, were also observed. The signals labeled 12, 15, and 20 could be assigned to hydrogens in the vicinity of the carbonyl group of benzoquinone or benzoquinone monoimine rings, while the signal 11 could be assigned to hydrogen in the vicinity of the monoimine group of the benzoquinone

Scheme 2. Boyland−Sims Rearrangement of Aniline and APS (top) Leading to *p*-Benzoquinone Monoime Units (Adapted from Ref 10)[a]

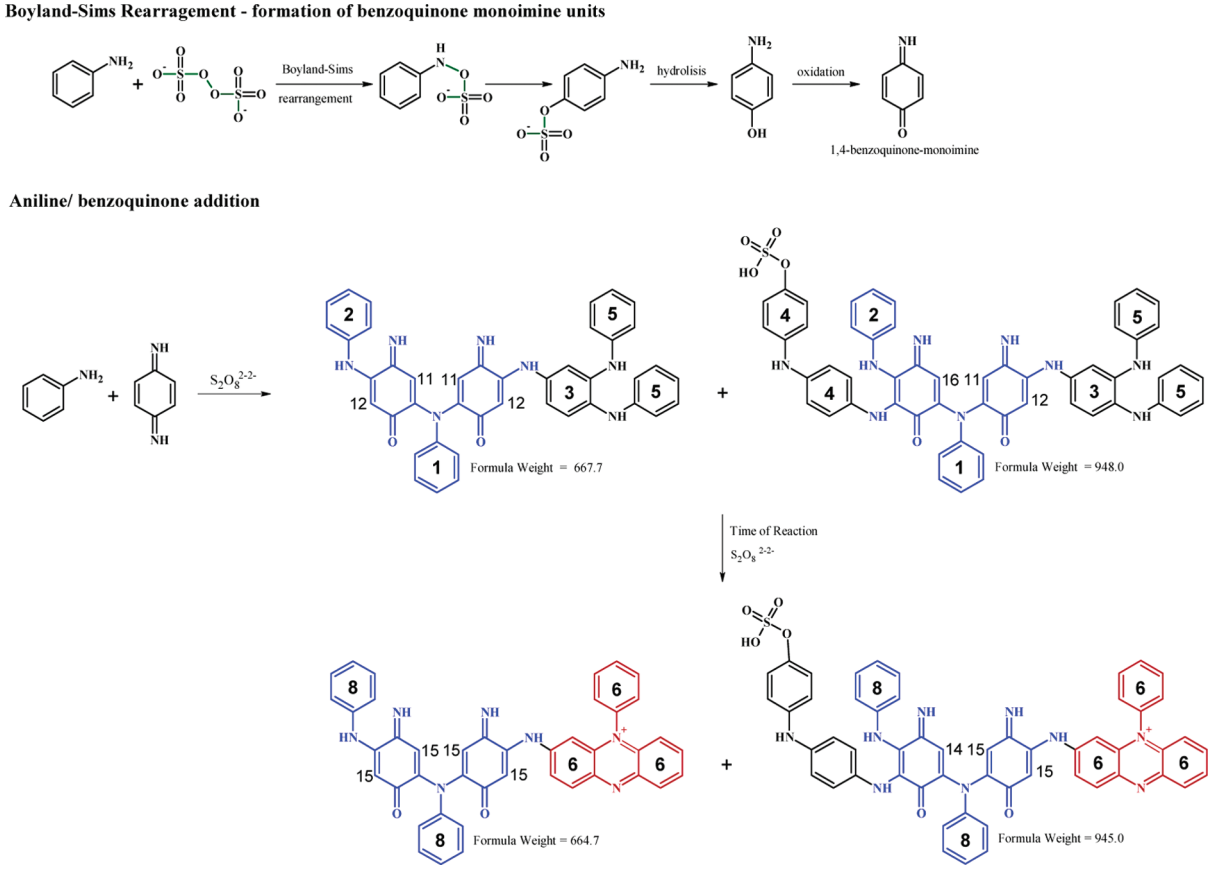

[a] The bottom displays the reaction between aniline and *p*-benzoquinone monoimine in the presence of APS in pH 3 buffer medium. The numbers refer to the assignments done to ^{1}H and ^{13}C (in parentheses) NMR peaks.

dx.doi.org/10.1021/jp111065m |*J. Phys. Chem. B* 2011, 115, 1368–1375

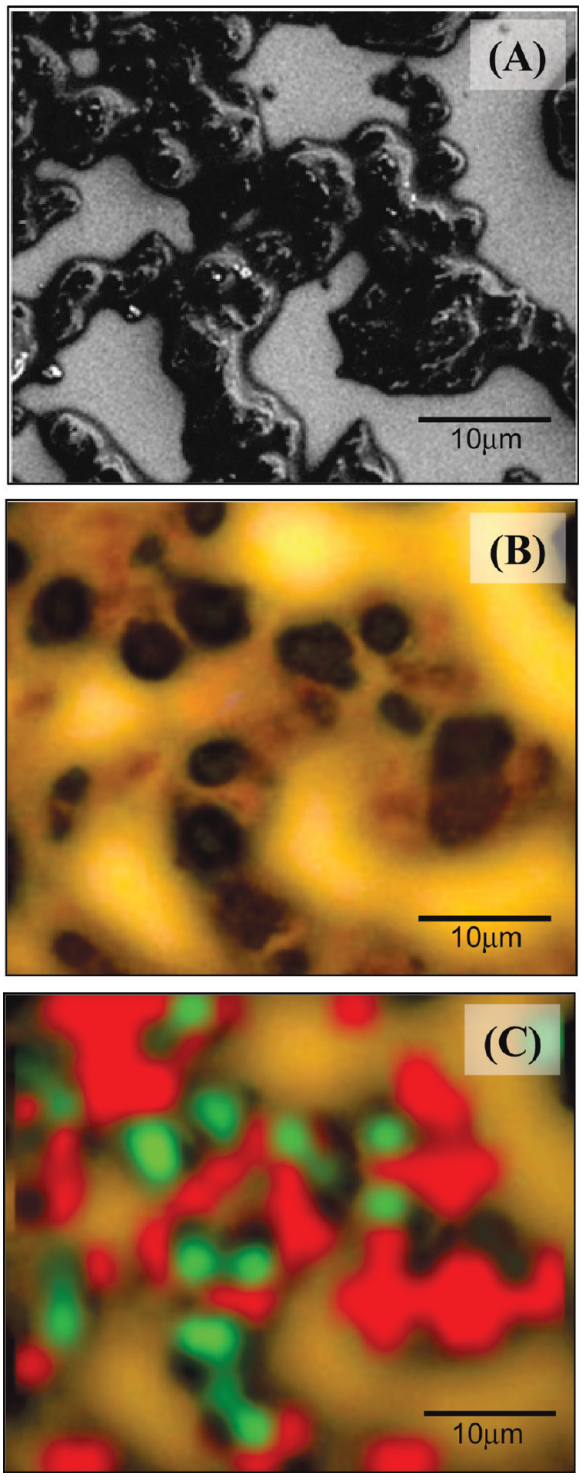

Figure 8. (A) SEM image (1000× magnification, 5.0 kV, and WD 8.7 mm), (B) optical image (100× magnification), and (C) Raman mapping at 633 nm exciting radiation monitoring the intensity of the Raman bands at ca. 1370 cm^{-1} (green region) and at ca. 1680 cm^{-1} (red region) at the same point of the T5.5 sample.

monoimine. The signals labeled 10 and 19 respectively in Figures 6 and 7 can be attributed to hydrogens of a benzoquinone ring, which suffered a single aniline addition.

Considering the vibrational and NMR data, we could assign the two main mass peaks observed. The peak at 663.5 m/z is consistent with macromolecules formed by five aniline residues and two *p*-benzoquinone monoimine residues, and the peak at 974.5 m/z to macromolecules formed by seven aniline residues, two *p*-benzoquinone monoimine residues, and one sulfate group. The structure of these macromolecules is presented in Scheme 2. For T5.5, the two compounds have primarily the 1,4-Michael-type reaction chromophore (in blue in Scheme 2). As the time of reaction increased, hydrolysis/oxidation of the imine group from the 1,4-benzoquinone monoimine moieties resulted in *p*-benzoquinone units. In addition, phenazine-like rings (in red in Scheme 2) will be formed by an internal cyclization of aniline residues coupled in the ortho position.[19] The products T22, T49, and T102 must differ from T5.5 and T171 in the degree of hydrolysis/oxidation of the imine groups and in the amount of phenazine-like segments.

In order to find a relation between the molecular structure and morphology, the T5.5 sample was analyzed by Raman mapping using the excitation line at 633 nm by monitoring the Raman bands at ca. 1370 and 1680 cm^{-1}. The results are shown in Figure 8. The intensity of the Raman band at ca. 1370 cm^{-1}, assigned to phenazine-like structures, generated the green regions in Figure 8C, while the intensity of 1680 cm^{-1} band, related to the stretching of carbonyl groups, yields the red regions. It is possible to observe in Figure 8B the presence of dark brown circular regions that can be associated to the spherical-like shape observed in the SEM image (Figure 8A). Interestingly, these dark brown circular regions could be correlated to the phenazine-like spectrum, showed as the green regions in Figure 8C. Conversely, the light brown region in Figure 8B could be correlated to carbonyl-like group spectrum, shown as red regions in Figure 8C that are associated with segments from the 1,4-Michael-type reaction between aniline and benzoquinone monoimine. These results suggest that phenazine-type segments are associated with the formation of the microspheres. These Raman mapping data corroborate our previous results where it was shown that the formation of PANI nanostructured on fibers is related to the presence of safranine-O or phenazine-type rings on PANI chains[25] and that the formation of nano/microstructured oligo/polyanilines is associated with the presence of the phenazine unit.[12,19,27]

4. CONCLUSION

This work demonstrated that the structures of the products formed in the reaction of aniline and APS (1:1 concentration ratio) using citrate/phosphate buffer solutions at pH 3 presented segments formed by 1,4-Michael reactions of aniline and *p*-benzoquinone monoimine. Specifically, our results showed that phenazine units were formed at later stages than segments from the 1,4-Michael-type reaction between aniline and benzoquinone monoimine. Our results rule out the formation of polyazane structures. Moreover, the presence of these segments indicates that the reaction of aniline and APS does not occur via oxidation resulting in head-to-tail chains at pH 3. Instead, it takes place via nucleophilic attack of aniline to APS, leading to benzoquinone monoimine units with different hydrolysis/oxidation degrees. Finally, our Raman mapping studies suggest that phenazine-like segments could be related to the formation of microspheres.

■ ASSOCIATED CONTENT

Ⓢ Supporting Information. Elemental analysis data for T5.5, T49, and T171, and FTIR spectra of TX samples and AnBzq.

This material is available free of charge via the Internet at http://pubs.acs.org.

AUTHOR INFORMATION

Corresponding Author
*E-mail: mlatempe@iq.usp.br. Tel.: + 55 11 3091 3853. Fax: + 55 11 3091 3890.

ACKNOWLEDGMENT

The authors acknowledge the Brazilian agencies CNPq, FAPESP, and FAPERJ for fellowship and financial support. The authors are also grateful to Dr. Luiz Henrique Catalani and Miss Vânia A. B. Bueno (IQ-USP) for HPLC measurements.

REFERENCES

(1) Fahlman, M.; Crispin, X.; Guan, H.; Li, S.; Smallfield, J. A. O.; Wei, Y.; Epstein, A. J. *Polym. Prepr.* **2000**, *41*, 1753–1754.
(2) Tallman, D. E.; Spinks, G.; Dominis, A.; Wallace, G. G. *J. Solid State Electrochem.* **2002**, *6*, 73–84.
(3) Higuchi, M.; Ikeda, I.; Hirao, T. *J. Org. Chem.* **1997**, *62*, 1072–1078.
(4) Virji, S.; Huang, J. X.; Kaner, R. B.; Weiller, B. H. *Nano Lett.* **2004**, *4*, 491–496.
(5) Virji, S.; Fowler, J. D.; Baker, C. O.; Huang, J. X.; Kaner, R. B.; Weiller, B. H. *Small* **2005**, *1*, 624–627.
(6) (a) Wei, Z.; Zhang, Z.; Wan, M. *Langmuir* **2002**, *18*, 917–921. (b) Wei, Z.; Wan, M. *Adv. Mater.* **2002**, *14*, 1314–1317.
(7) Ćirić-Marjonović, G.; Holclajtner-Antunović, I.; Mentus, S.; Banjuk-Bogdanović, D.; Ješić, D.; Manojlović, D.; Trifunović, S.; Stejskal, J. *Synth. Met.* **2010**, *160*, 1463–1473.
(8) do Nascimento, G. M.; Kobata, P. Y. G.; Temperini, M. L. A. *J. Phys. Chem. B* **2008**, *112*, 11551–11557.
(9) Venancio, E. C.; Wang, P.-C.; MacDiarmid, A. G. *Synth. Met.* **2006**, *156*, 357–369.
(10) Surwade, S. P.; Dua, V.; Manohar, N.; Manohar, S. K.; Beck, E.; Ferraris, J. P. *Synth. Met.* **2009**, *159*, 445–455.
(11) Trchová, M.; Šeděnková, I.; Konyushenko, E. N.; Stejskal, J.; Holler, P.; Ćiric-Marjanović, G. *J. Phys. Chem. B* **2006**, *110*, 9461–9468.
(12) Zujovic, Z. D.; Zhang, L.; Bowmaker, G. A.; Kilmartin, P. A.; Travas-Sejdic, J. *Macromolecules* **2008**, *41*, 3125–3135.
(13) Ćiric-Marjanović, G.; Trchová, M.; Stejskal, J. *J. Raman Spectrosc.* **2008**, *39*, 1375–1387.
(14) Sedenkova, I.; Trchova, M.; Stejskal, J.; Bok, J. *Appl. Spectrosc.* **2007**, *61*, 1153–1162.
(15) Bax, A.; Subramanian, S. *J. Magn. Reson.* **1986**, *67*, 565–569.
(16) Johnson, C. S. *Prog. NMR Spectrosc.* **1999**, *34*, 203–256.
(17) Beckmann, U.; Dietrich, W.; Radeglia, R. *J. Magn. Reson.* **1999**, *137*, 132–137.
(18) Braunschweiler, L.; Ernst, R. R. *J. Magn. Reson.* **1983**, *53*, 521–528.
(19) Sapurina, I.; Stejskal, J. *Polym. Int.* **2008**, *57*, 1295–1325.
(20) Zujovic, Z. D.; Laslau, C.; Bowmaker, G. A.; Kilmartin, P. A.; Webber, A. L.; Brown, S. P.; Travas-Sejdic, J. *Macromolecules* **2010**, *43*, 662–670.
(21) Ding, Z.; Sanchez, T.; Labouraiu, A.; Iyer, S.; Larson, T.; Currier, R.; Zhao, Y.; Yang, D. *J. Phys. Chem. B* **2010**, *114*, 10337–10346.
(22) Laslau, C.; Zujovic, Z. D.; Zhang, L.; Bowmaker, G. A.; Travas-Sejdic, J. *Chem. Mater.* **2009**, *21*, 954–962.
(23) Kříž, J.; Starovoytova, L.; Trchová, M.; Konyushenko, E. N.; Stejskal, J. *J. Phys. Chem. B* **2009**, *113*, 6666.
(24) do Nascimento, G. M.; Constantino, V. R. L.; Landers, R.; Temperini, M. L. A. *Macromolecules* **2004**, *37*, 9373–9385.
(25) do Nascimento, G. M.; Silva, C. H. B.; Temperini, M. L. A. *Macromol. Rapid Commun.* **2006**, *27*, 255–259.
(26) Sestrem, R. H.; Ferreira, D. C.; Landers, R.; Temperini, M. L. A.; do Nascimento, G. M. *Eur. Polym. J.* **2010**, *4*, 484–493.
(27) Stejskal, J.; Sapurina, I.; Trichová, M.; Konyushenko, E. N.; Holler, P. *Polymer* **2006**, *47*, 8255–8262.